Data on sputtering and hydrogen retention of Be and Be alloy

Daiji Kato
National Institute for Fusion Science

Contents

- Sputtering yield database at NIFS
  - NIFS database (SPUTY)
  - Web-site for compilation of Eckstein's TRIM.SP calculations (IPP-report)
- Review on sputtering yield data research including Japanese activities
- Review on hydrogen retention study including Japanese activities

SPUTY
sputtering yields for monoatomic solids (amorphous target, normal incidence only)

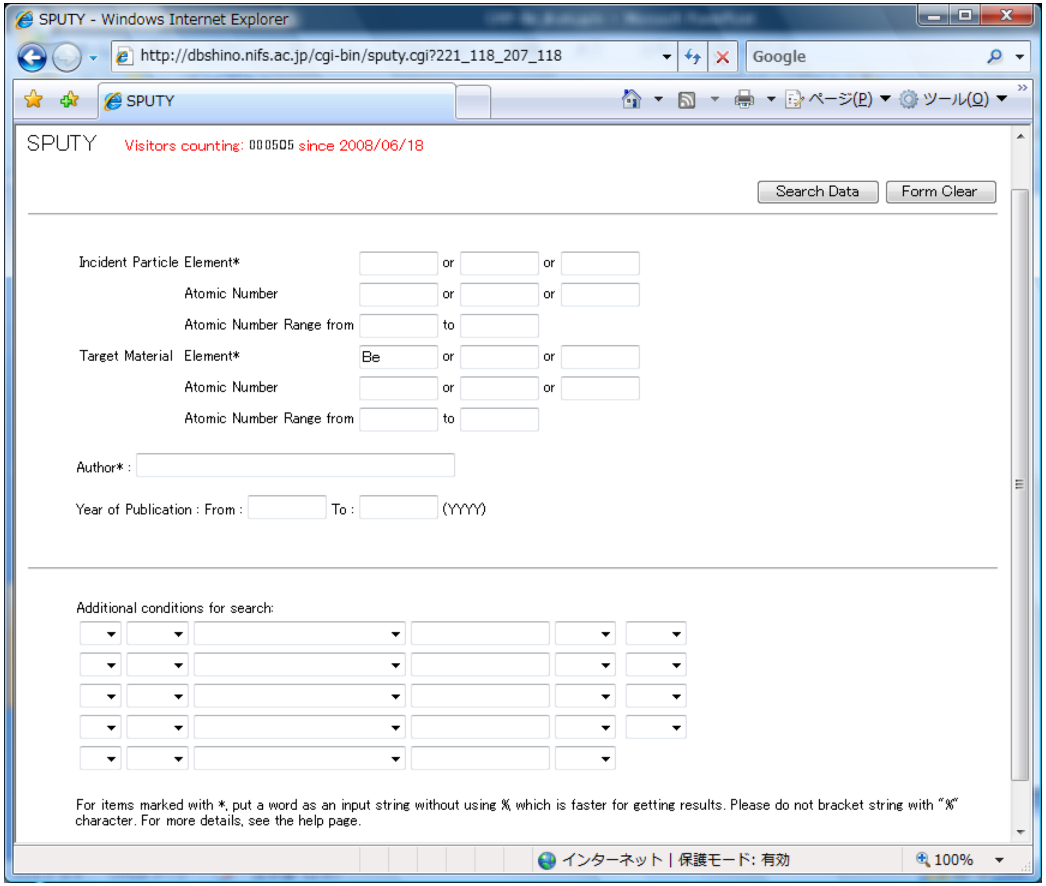

http://dbshino.nifs.ac.jp

Found Result in SPUTY - Windows Internet Explorer
http://dbshino.nifs.ac.jp/cgi-bin/sea_sputy.cgi?221_118_207_
Google
Found Result in SPUTY
ページ(P)
ツール(O)
[Help]
Found Result in SPUTY
Found 35 Title(s)
All Data List 35 records found
AR --> BE 3 records found
BE --> BE 4 records found
D --> BE 5 records found
H --> BE 5 records found
HE --> BE 6 records found
HE-3 --> BE 1 records found
KR --> BE 3 records found
NE --> BE 3 records found
O --> BE 1 records found
T --> BE 1 records found
XE --> BE 3 records found
ページが表示されました
インターネット | 保護モード: 有効
100%

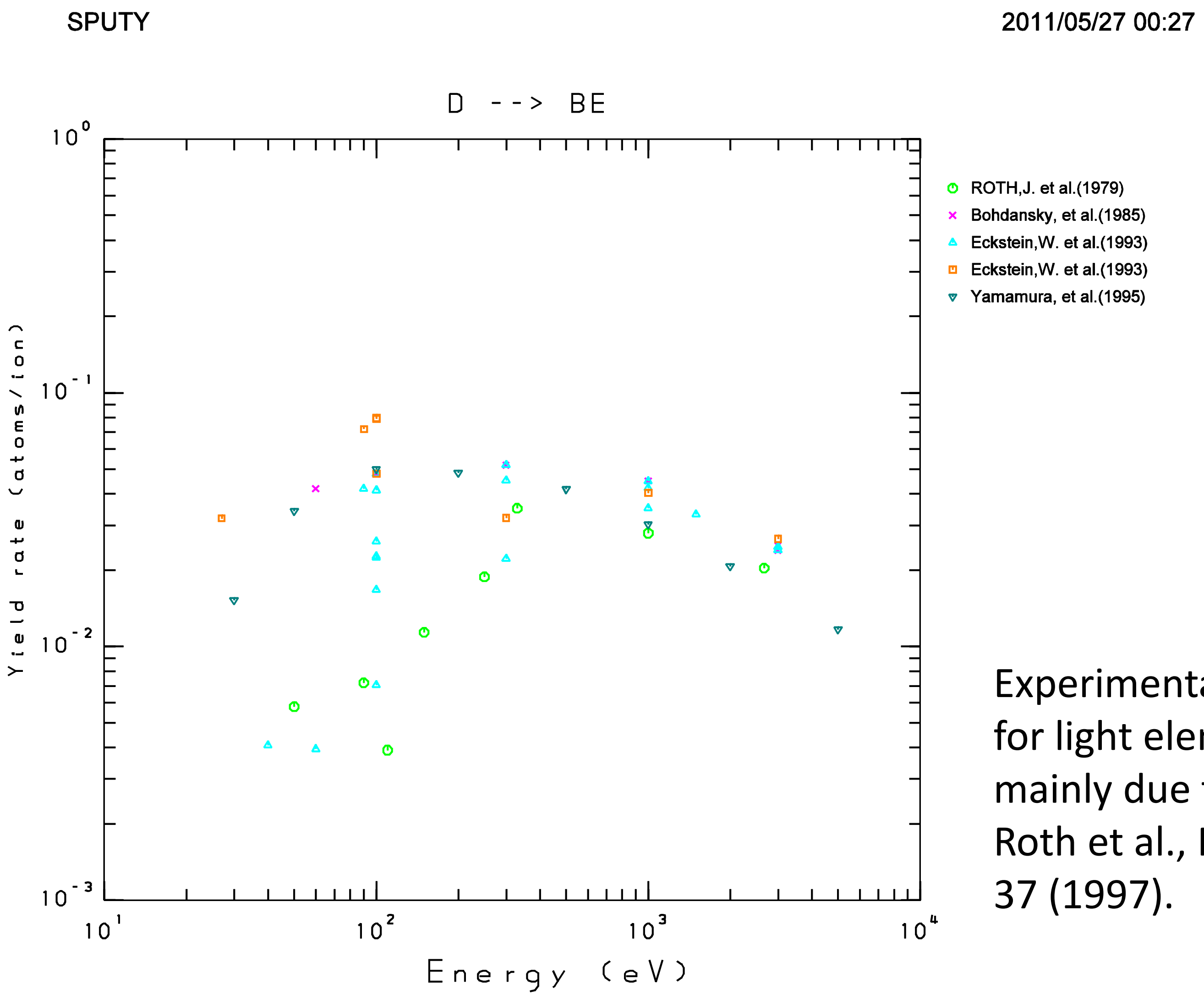

Experimental data are scattered for light element projectiles. It is mainly due to surface oxidation. Roth et al., Fusion Eng. Design 37 (1997).

NIFS-DATA-23 (1995)

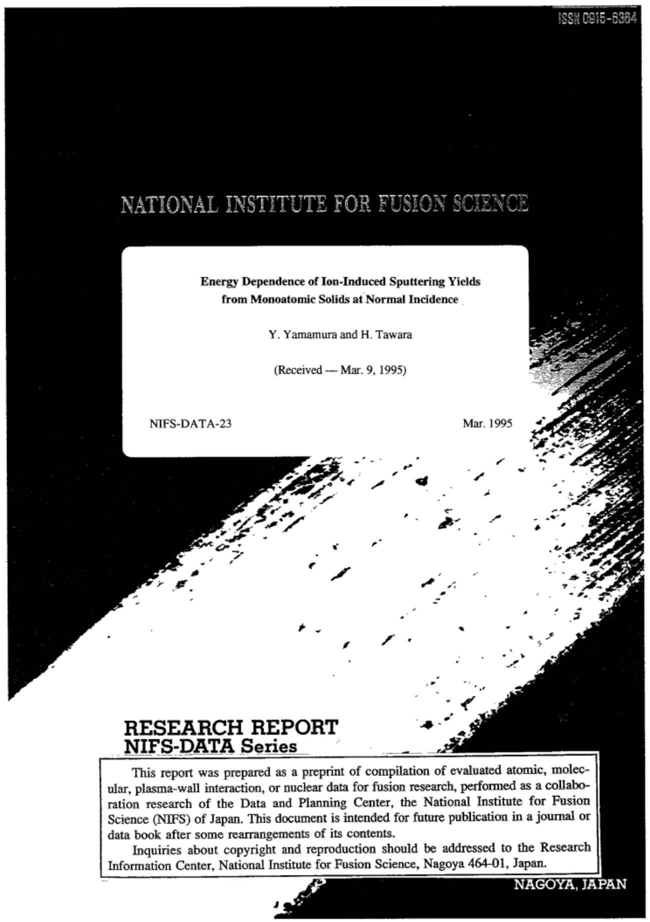
ISSN 0915-6364

NATIONAL INSTITUTE FOR FUSION SCIENCE

Energy Dependence of Ion-Induced Sputtering Yields from Monoatomic Solids at Normal Incidence

Y. Yamamura and H. Tawara

(Received — Mar. 9, 1995)

NIFS-DATA-23 Mar. 1995

RESEARCH REPORT
NIFS-DATA Series

This report was prepared as a preprint of compilation of evaluated atomic, molecular, plasma-wall interaction, or nuclear data for fusion research, performed as a collaboration research of the Data and Planning Center, the National Institute for Fusion Science (NIFS) of Japan. This document is intended for future publication in a journal or data book after some rearrangements of its contents.

Inquiries about copyright and reproduction should be addressed to the Research Information Center, National Institute for Fusion Science, Nagoya 464-01, Japan.

NAGOYA, JAPAN

ENERGY DEPENDENCE OF ION-INDUCED SPUTTERING YIELDS FROM MONOATOMIC SOLIDS AT NORMAL INCIDENCE

Yasunori Yamamura[a)] and Hiro Tawara

National Institute for Fusion Science, Chigusa-ku

Nagoya 464-01, Japan

Abstract

The yields of the ion-induced sputtering from monoatomic solids at normal incidence for various ion-target combinations are presented graphically as a function of the incident ion energy. In order to fill the lack of the experimental data, the sputtering yields are also calculated by the Monte Carlo simulation code ACAT for some ion-target combinations. Each graph shows available experimental data points and the ACAT data, together with the sputtering yields calculated by the present empirical formula, whose parameters are determined by the best-fit to available data.

Web site of Eckstein’s data compilation

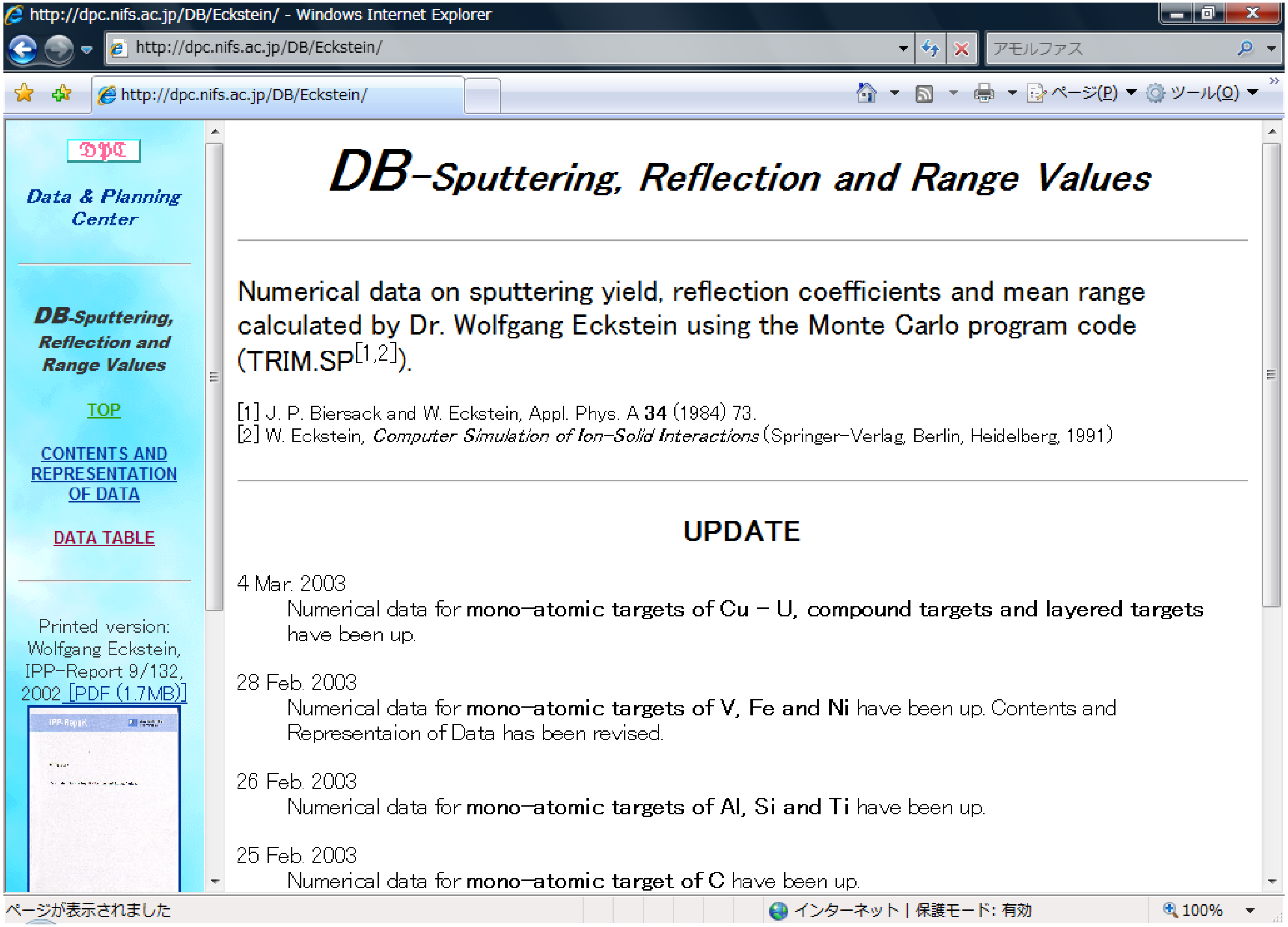

http://dpc.nifs.ac.jp/DB/Eckstein/

Ion-target combinations in the database:
Monoatomic target (H,D,T,He,Be,N,O,Ne,Ar – Be)
Compound target (O – BeO)

```
% sputtering yield : D -> Be
% z1= 1, m1=  2.01, z2= 4, m2=  9.01, sbe=3.38 eV, rho=1.80 g/cm**3
% ef=0.95 eV, esb=1.00 eV, kk0=kk0r=2, kdee1=kdee2=3, ipot=ipotr=1 (KrC)
% ca=1.00
% program : trvmc, IPP 9/82
% ne=21, na=10
%
```

% e0	0	15	30	45	55	60	65	70	75	80	85	87
10	4.13e-6	4.30e-6	4.56e-6									
11	2.61e-5	3.05e-5	3.15e-5	2.69e-5	1.86e-5		1.00e-5		3.67e-6	8.00e-7	5.00e-7	
12	9.29e-5	1.07e-4	1.25e-4	1.14e-4	8.71e-5	6.81e-5	5.37e-5		2.31e-5	1.39e-5	9.62e-6	
13	2.32e-4	2.67e-4	3.47e-4	3.16e-4	2.61e-4	2.10e-4	1.62e-4		7.67e-5	4.78e-5	3.18e-5	
14	4.65e-4	5.50e-4	6.90e-4	6.91e-4	5.92e-4		3.92e-4		1.91e-4	1.20e-4	7.85e-5	
15	8.10e-4	9.42e-4	1.21e-3	1.29e-3	1.12e-3	9.82e-4	7.97e-4		4.11e-4	2.57e-4	1.65e-4	
17	1.73e-3	2.02e-3	2.60e-3	3.03e-3	2.92e-3		2.29e-3		1.25e-3	7.67e-4	4.62e-4	
20	3.64e-3	4.19e-3	5.46e-3	7.03e-3	7.46e-3	7.12e-3	6.59e-3		3.76e-3	2.14e-3	1.16e-3	
25	7.30e-3	8.25e-3	1.11e-2	1.57e-2	1.87e-2	1.94e-2	1.85e-2		1.08e-2	5.51e-3	2.51e-3	
30	1.08e-2	1.22e-2	1.69e-2	2.54e-2	3.25e-2	3.58e-2	3.46e-2		2.07e-2	1.02e-2	3.82e-3	
40	1.68e-2	1.90e-2	2.64e-2	4.34e-2	6.08e-2		7.17e-2		4.54e-2	2.12e-2	5.91e-3	
50	2.09e-2	2.40e-2	3.45e-2	5.78e-2	8.53e-2	9.88e-2	1.07e-1		7.40e-2	3.23e-2	7.37e-3	
70	2.63e-2	3.04e-2	4.43e-2	7.94e-2	1.19e-1		1.60e-1		1.28e-1	5.90e-2	9.51e-3	
100	3.10e-2	3.59e-2	5.42e-2	9.78e-2	1.49e-1	1.80e-1	2.13e-1		2.00e-1	1.01e-1	1.27e-2	
140	3.32e-2	3.94e-2	6.11e-2	1.08e-1	1.68e-1		2.48e-1		2.71e-1	1.60e-1	1.82e-2	
200	3.51e-2	4.03e-2	6.32e-2	1.14e-1	1.77e-1	2.20e-1	2.68e-1		3.42e-1	2.43e-1	2.93e-2	
300	3.44e-2	4.20e-2	6.34e-2	1.12e-1	1.75e-1	2.12e-1	2.72e-1		3.91e-1	3.42e-1	5.71e-2	
500	3.24e-2	3.85e-2	5.82e-2	1.04e-1	1.50e-1	1.98e-1	2.57e-1		4.08e-1	4.39e-1	1.38e-1	
1000	2.53e-2	2.96e-2	4.37e-2	7.80e-2	1.25e-1	1.54e-1	2.06e-1		3.65e-1	4.59e-1	3.34e-1	
2000	1.76e-2											
3000	1.25e-2		2.02e-2	3.43e-2		7.29e-2		1.29e-1		2.89e-1	4.59e-1	3.18e-1

Eckstein, *Sputtering by Particle Bombardment* (Springer, 2007)

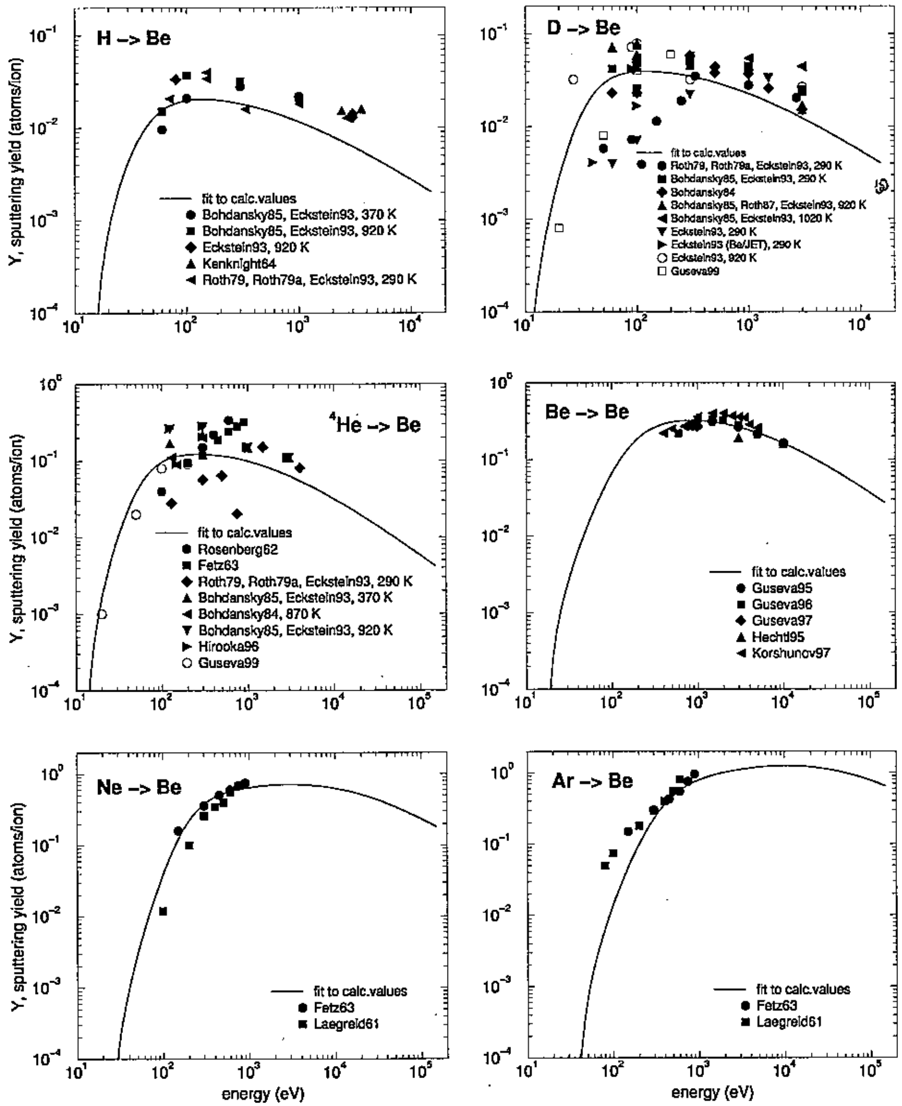

Fig. 5. Energy dependence of sputtering yields of Be for bombardment at normal incidence [47] with H [27, 48–51], D [16, 27, 48, 50–53], ^{4}He [16, 17, 48, 50, 51, 54–57], Be [58–62], Ne [55, 63] and Ar [55, 63]. Several authors in one line mean the same data in different publications

Eckstein, *Sputtering by Particle Bombardment* (Springer, 2007)

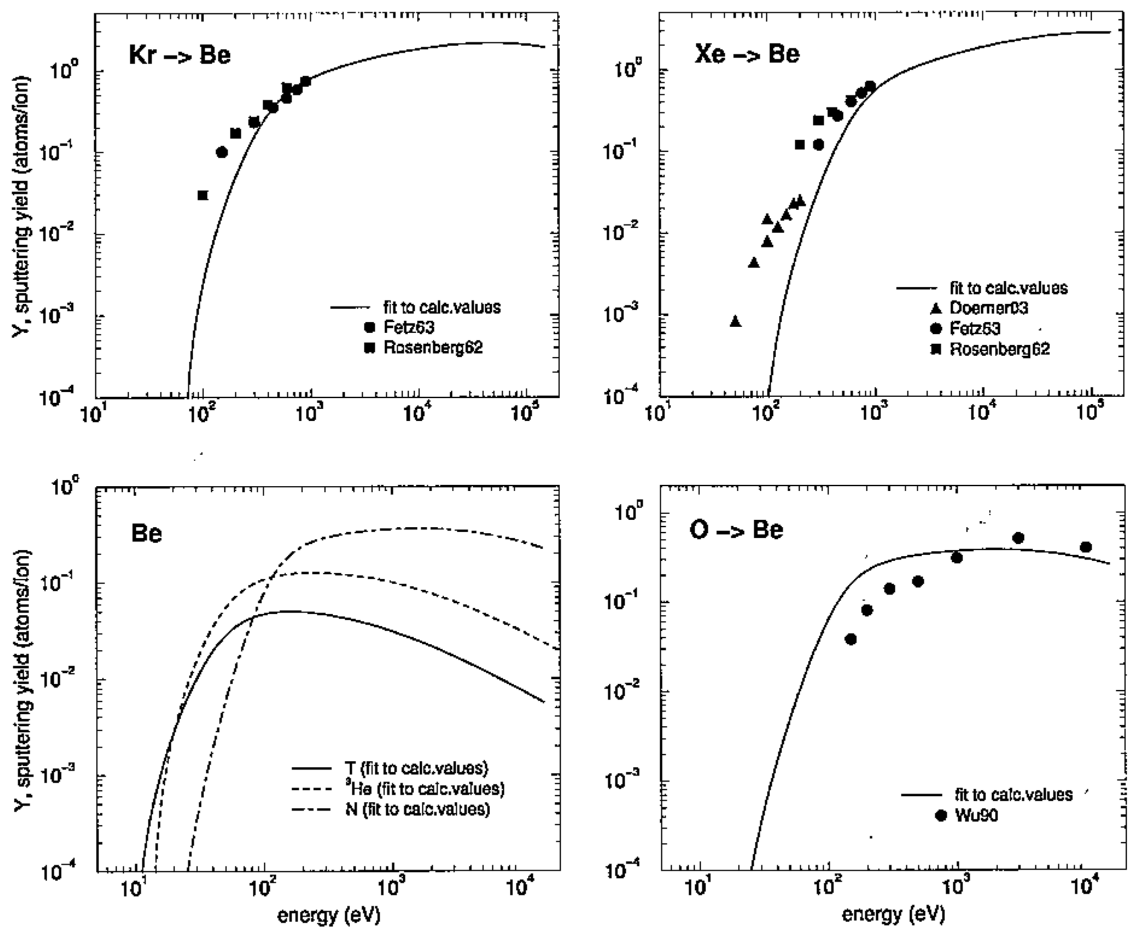

Fig. 6. Energy dependence of sputtering yields of Be for bombardment at normal incidence with Kr [54, 55], Xe [18, 54, 55], T and ^{3}He and N, and O [64]

Material mixing effect is significant in cases that incident particles make compound with target

Wu et al., JNM176-177 (1990)

Weight loss method

Partial sputtering yield of BeO

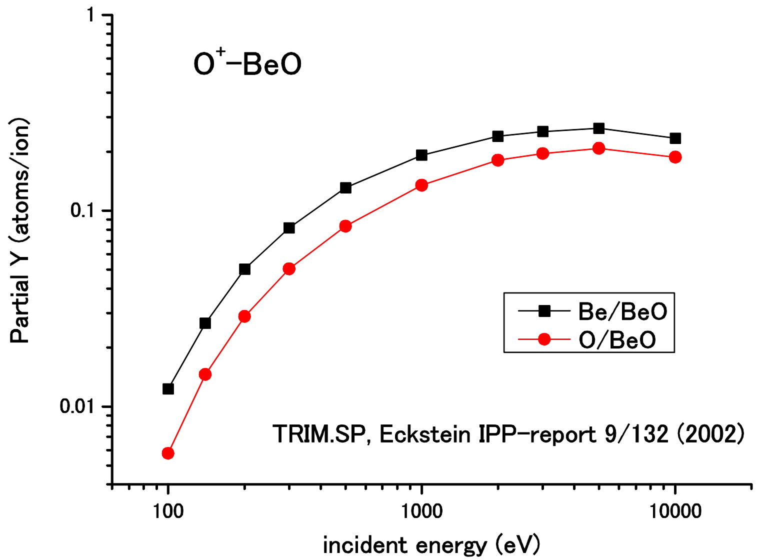

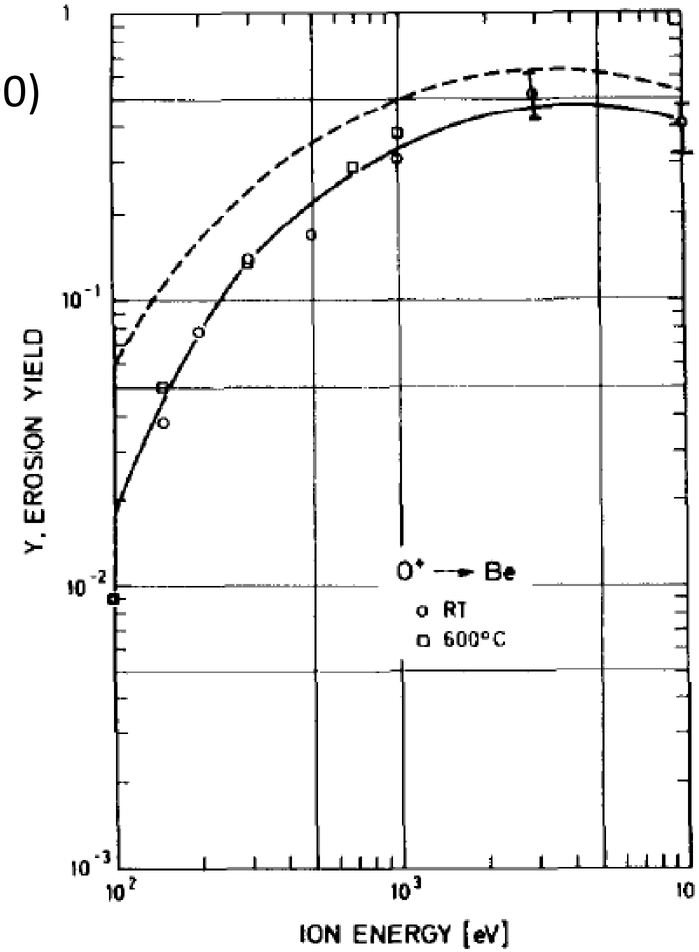

Fig. 1 The measured erosion yields of beryllium exposed to oxygen, as a function of energy: dashed line O → Be, solid line O → BeO TRIM-SP code.

Erosion of Be wall in ITER affected by co-deposition of C and W

$Be^+ \rightarrow$ Be, Be-C, Be-W

Korshunov et al., JAERI-Conf. 98-001 (1998)

Weight loss method

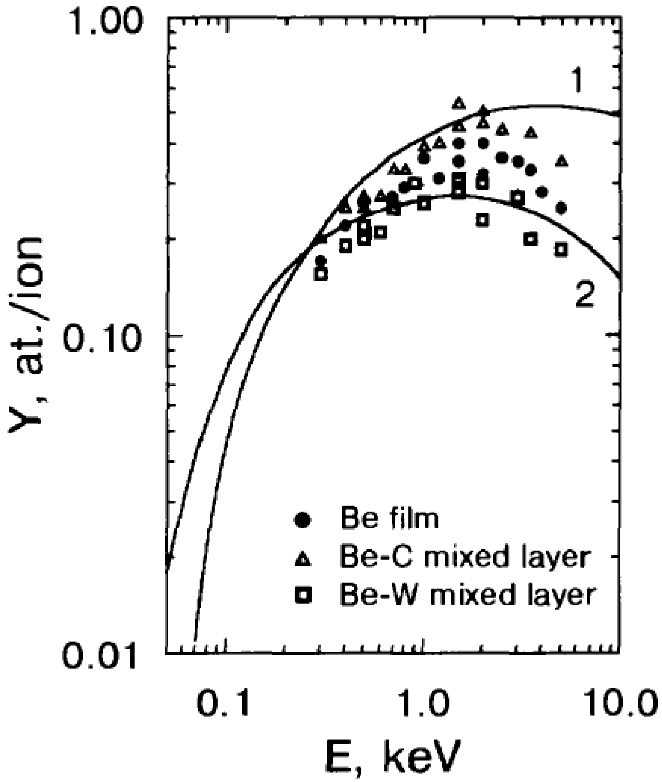

Figure 6. Experimental sputtering yield data for Be-C, Be-W mixed layers and for Be deposited films in comparison with experimental energy dependences of the self-sputtering yields for carbon (curve 1) and beryllium (curve 2).

Be-D

Mixed layers co-deposited on Si substrate by simultaneous sputtering of pair targets (Be+C and Be+W).

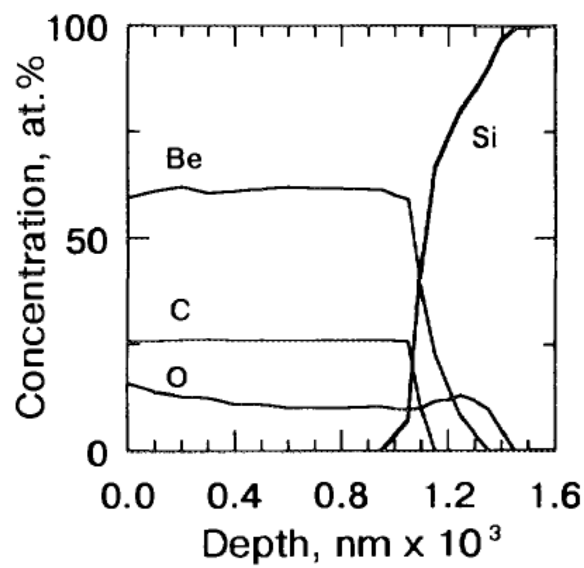

Figure 3. The depth distribution of elements in the Be-C mixed layer deposited on Si collector.

Sputtering yield may depend on fluence.

Oscillatory variations of yield with fluence were predicted for light element targets bombarded by heavy projectiles, e.g. W → Be. Eckstein, NIMB171 (2000).

Exp. SIMS measurement of partial sputtering yield of Cs^+ ion implanted on Be. Sielanko et al., Vaccum 70 (2003).

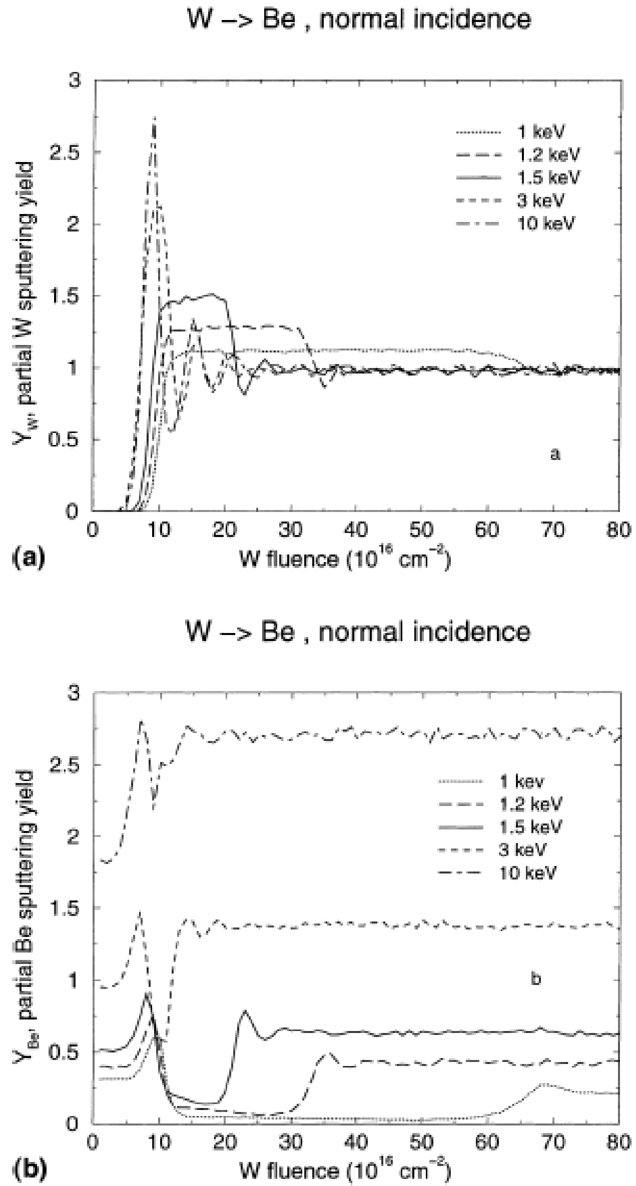

Fig. 1. Partial sputtering yields versus incident W fluence. Be is bombarded with 1, 1.2, 1.5, 3 and 10 keV W at normal incidence. (a) W partial sputtering yield, (b) Be partial sputtering yield.

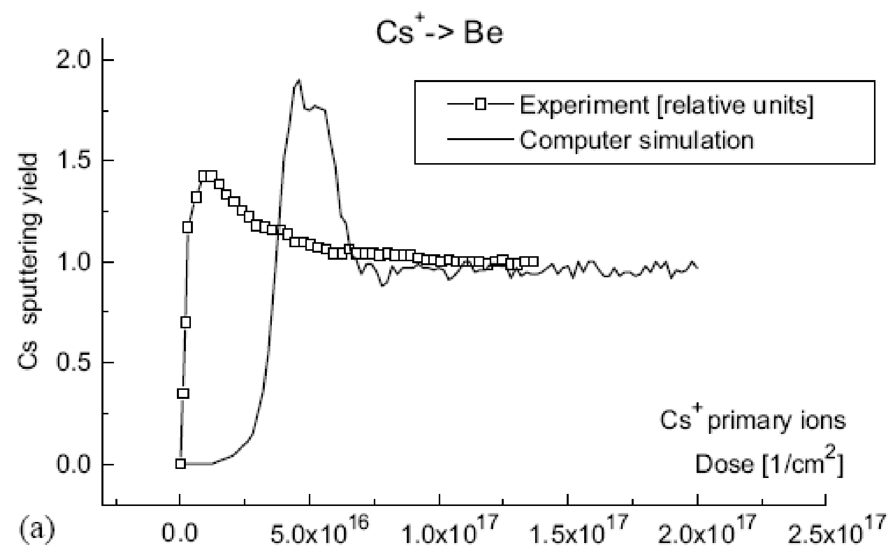

Eckstein, *Sputtering by Particle Bombardment* (Springer, 2007)

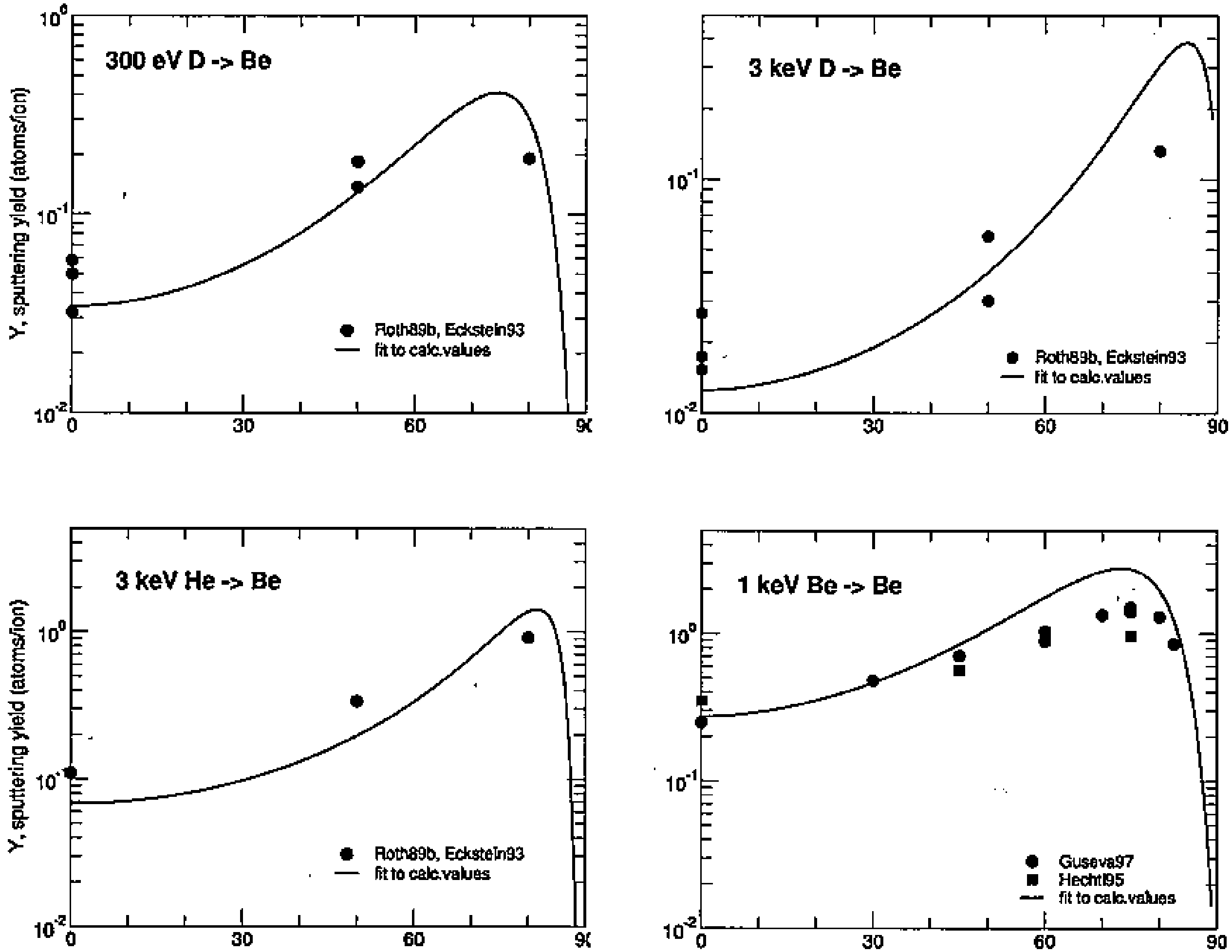

Incident angle

Temperature dependence of sputtering yield of Be

Radiation induced sublimation is observed. In the Figure, incident ion flux is 6×10^{19} /m^2/s. For low energy bombardment, yield enhancement is attributed to surface transition from oxide to clean Be.

Roth et al., Fusion Eng. Design 37 (1997).

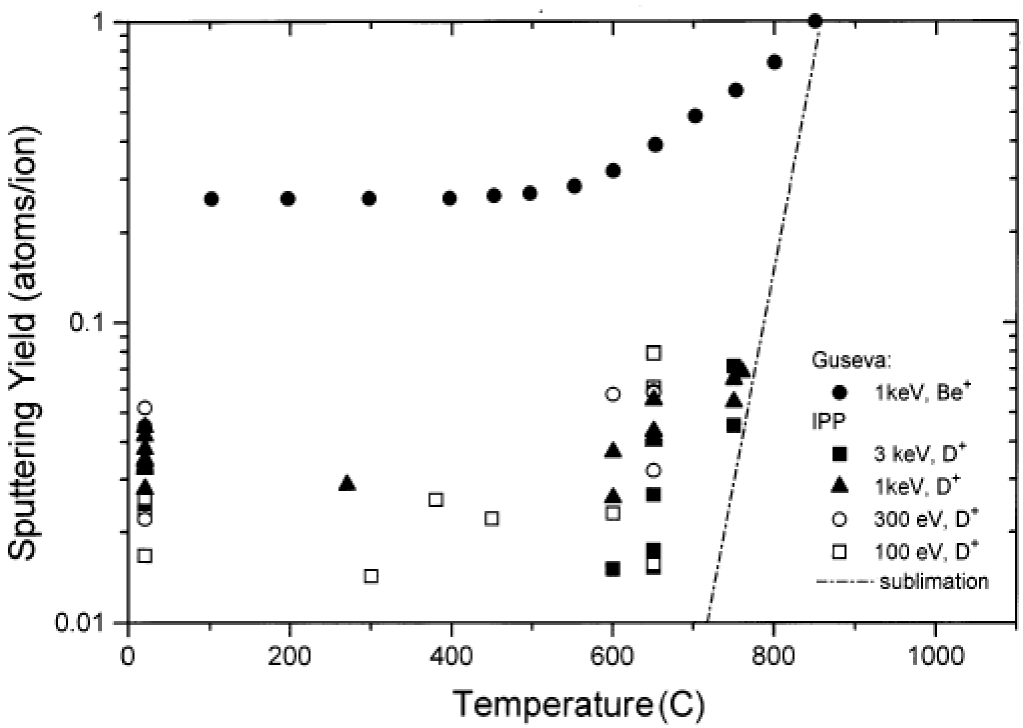

Fig. 14. Sputtering yield vs. the Be target temperature for 0.1, 0.3, 1 and 3 keV D and 1 keV Be bombardment at normal incidence [6,16,17,39].

Sputtering by multi-species impact

Besides plasma ions, impurities, e.g. C, O, metals, and coolant inert gas atoms, would affect sputtering properties.

It was found that non-recycling impurity, e.g. C, reduced erosion of Be substantially, called as “carbon poisoning”.

Roth et al., Fusion Eng. Design 37 (1997).

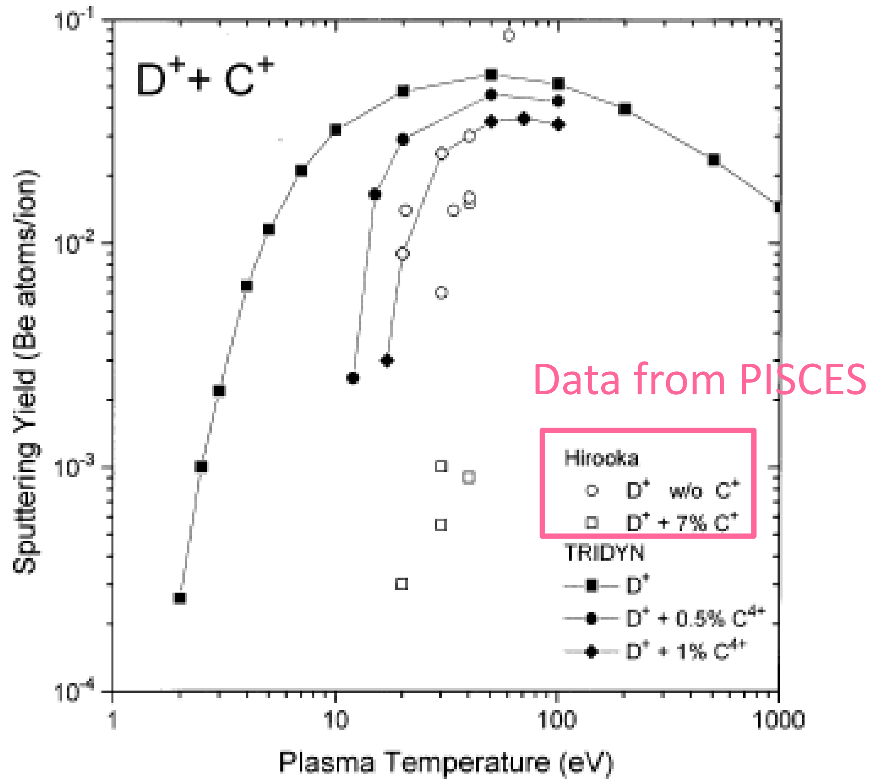

Fig. 19. Sputtering yield vs. the (electron) plasma temperature for a Maxwellian distribution of D and C projectiles bombarding Be. Experimental data for 400 eV D [25,53]. Calculated values for several impurity levels of C [38].

Available data and knowledge-base

- Monoatomic and some mixed-materials targets, e.g. Be-W, Be-C, Be-O.
- Incident energy dependence (> 10 eV).
- Incident angle dependence.
- Target temperature dependence, with emphasis on surface composition change.
- Multi species-impact, with emphasis on plasma impurity effects.
- Energy-angular distribution of sputtered particles. Data can be obtained by MC simulation and Thompson formula for energy distribution for normal incidence.

Not clear, further investigation is necessary

- Low energy (< 10 eV) data.
- Energy-angular distribution of sputtered particles.
- Identification of sputtered species: atoms, molecules, clusters.
- Ro-vibration states of molecular species, electronic excited states.

Molecular dynamics simulation of erosion of a-C:H layer co-deposited with Be

Kaoru Ohya (Tokushima Univ., Japan), private communication

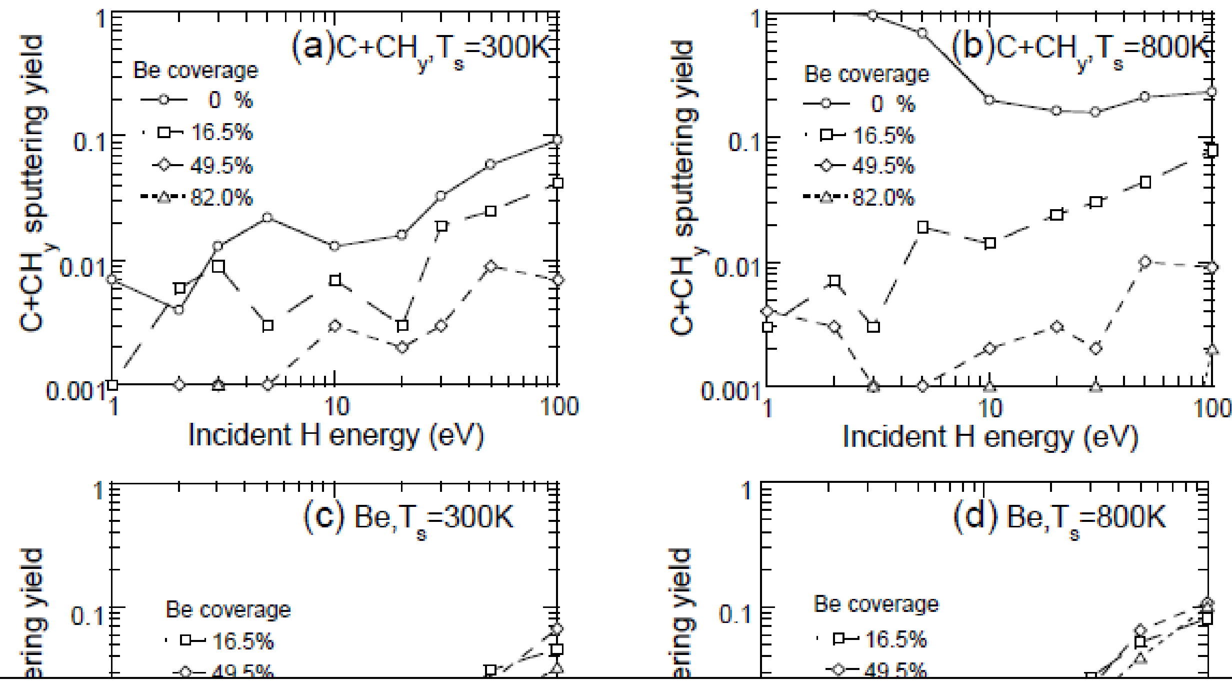

Erosion mitigation is attributed to formation of strong Be-C and Be-H compound at surface layers. The erosion mitigation has been observed in C targets exposed to Be-seeded plasma in PISCES-B experiment.

percentage of coverage. The target temperatures are 300 K (a and c) and 800 K (b and d).

Hydrogen isotope retention in Be

- Review by Anderl et al., JNM 273 (1999).
- Since experimental studies have been performed intensively, data are available in literatures.
- Identification of trap sites may need further investigation.
- Database development has been undertaken at NIFS, but not updated.

Ishimoto et al., Plasma-Wall Interactions Data Compendium-3, NIFS-MEMO-42 (2004)

8 keV D_2^+ (4 keV D^+), flux 1e+18 D/m^2/s, temperature 300K
Sintered Be (Nilaco)
TDS (1K/s, 2-3 hours after implantation)
Yoshida et al., JNM233-237 (1996)

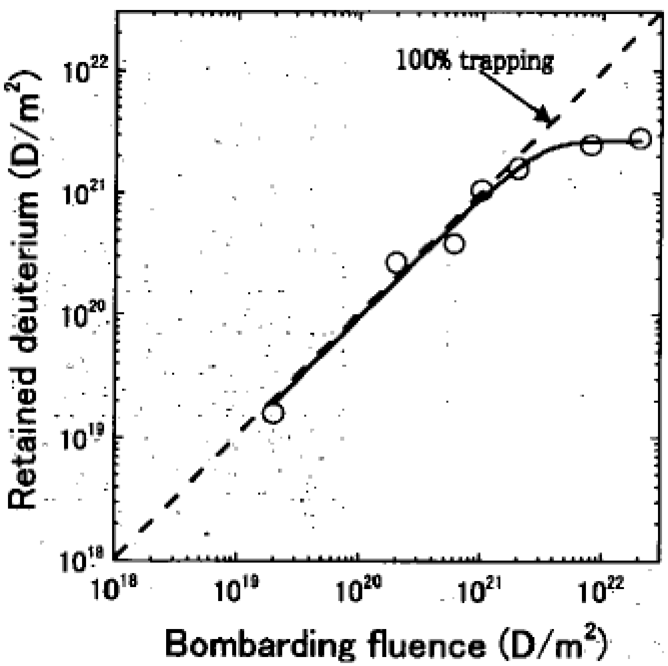

x(D/m^2)	y(D/m^2)
2.0E+19	1.6E+19
2.0E+20	2.7E+20
6.0E+20	3.8E+20
1.0E+21	1.1E+21
2.0E+21	1.6E+21
8.0E+21	2.5E+21
2.0E+22	2.8E+21

$$y = A_1 \tanh(x/A_2)$$

$$A_1 = 2.6676 \times 10^{21}$$

$$A_2 = 2.8210 \times 10^{21}$$

$$(x = 2 \times 10^{19} - 2 \times 10^{22}\ \mathrm{D/m^2})$$

Ishimoto et al., Plasma-Wall Interactions Data Compendium-3, NIFS-MEMO-42 (2004)

9 keV D^+, flux 1e+19 $D/m^2/s$, temperature 300K
Sintered Be (1 wt% BeO)
SIMS
Alimov et al., JNM241-243 (1997)

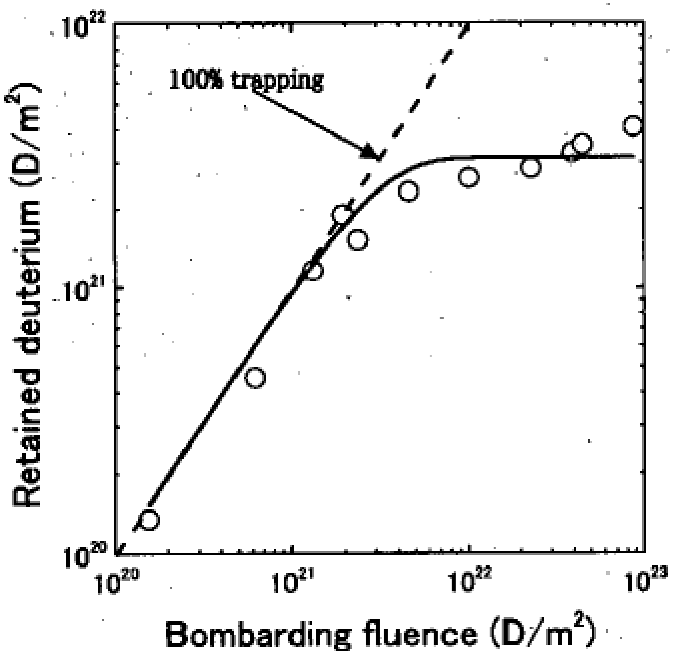

x(D/m²)	y(D/m²)
1.5E+20	1.3E+20
6.2E+20	4.6E+20
1.3E+21	1.2E+21
1.9E+21	1.9E+21
2.4E+21	1.5E+21
4.6E+21	2.3E+21
1.0E+22	2.6E+21
2.3E+22	2.8E+21
3.9E+22	3.3E+21
4.5E+22	3.5E+21
8.7E+22	4.1E+21

$$y = A_1 \tanh(x/A_2)$$

$$A_1 = 3.1282 \times 10^{21}$$

$$A_2 = 3.1735 \times 10^{21}$$

$$(x = 1 \times 10^{20} - 1 \times 10^{23} \text{ D/m}^2)$$

Ishimoto et al., Plasma-Wall Interactions Data Compendium-3, NIFS-MEMO-42 (2004)

3 keV D_3^+ (1 keV D^+), flux 1e+20 D/m^2/s , temperature 300K
Sintered Be (Brush Wellman)
TDS (7K/s)
Haasz et al., JNM241-243 (1997)

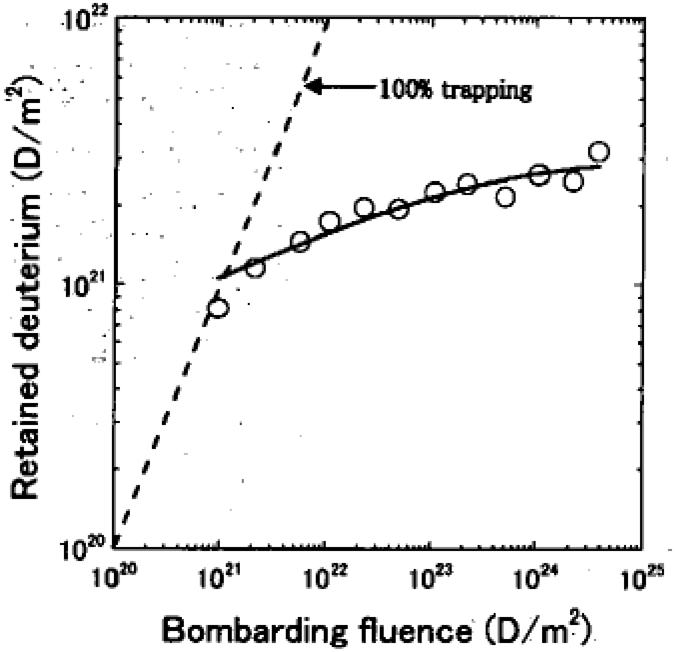

x(D/m^2)	y(D/m^2)
9.5E+20	8.1E+20
2.1E+21	1.2E+21
5.6E+21	1.5E+21
1.1E+22	1.7E+21
2.2E+22	2.0E+21
4.8E+22	1.9E+21
1.1E+23	2.2E+21
2.2E+23	2.4E+21
5.0E+23	2.2E+21
1.0E+24	2.6E+21
2.2E+24	2.5E+21
3.8E+24	3.2E+21

$$y = A_1 \tanh(x/A_2)^p$$
$$A_1 = 2.948 \times 10^{21}$$
$$A_2 = 1.5085 \times 10^{23}$$
$$p = 0.19387$$
$$(x = 1\times10^{21} - 3\times10^{24}\ \mathrm{D/m^2})$$

Typical thermal desorption spectra from Be samples bombarded by D ions at RT

Lower temperature (500-600 K) peaks are responsible for bulk of hydrogen retention at higher fluences. These peaks (disappear in high temperature above 373 K irradiations) were attributed to amorphous hydride formation in surface layers by Wilson, and to radiation damage traps or bubbles by Haasz.

Yoshida et al. (1996)

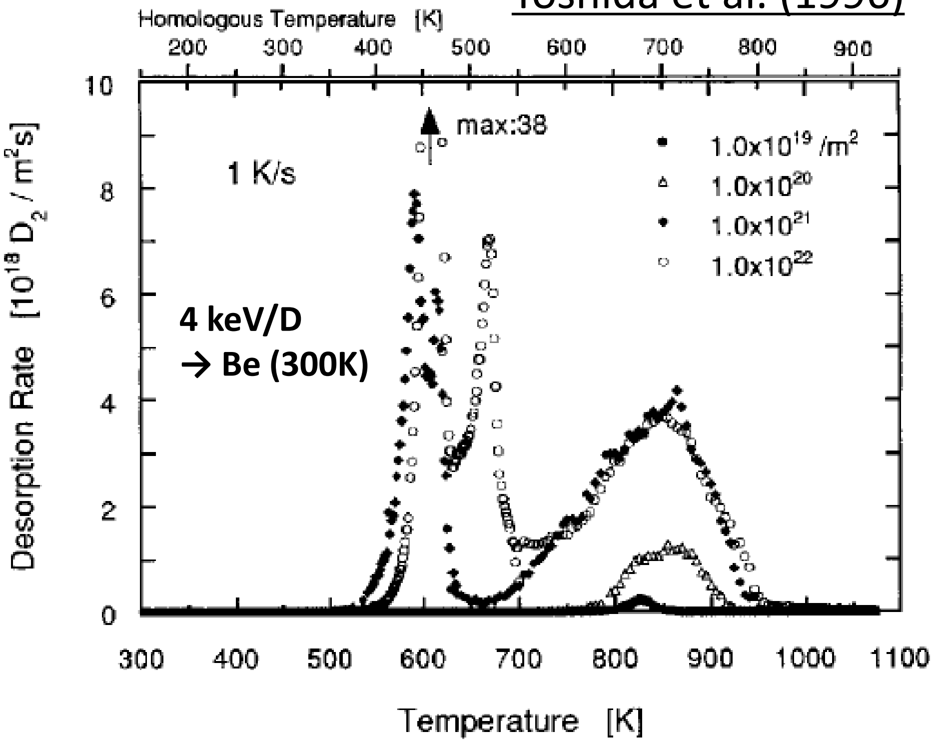

Haasz et al. (1997)

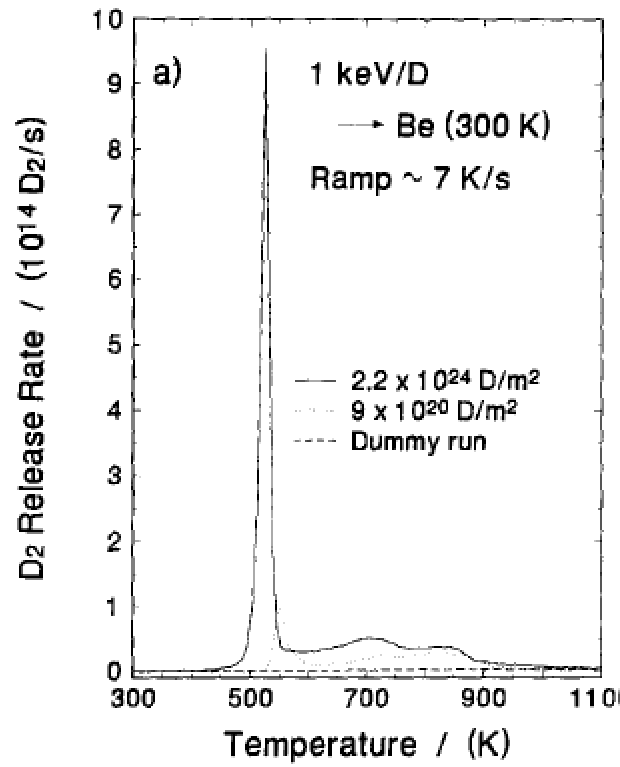

Thermal desorption spectra variation with irradiation temperature

Ha and Hb: loosely bounded to bubbles
Hc: trapped in mono-vacancy and small vacancy clusters
Hd: trapped in bubbles

<u>Yoshida et al., JNM233-237 (1996)</u>

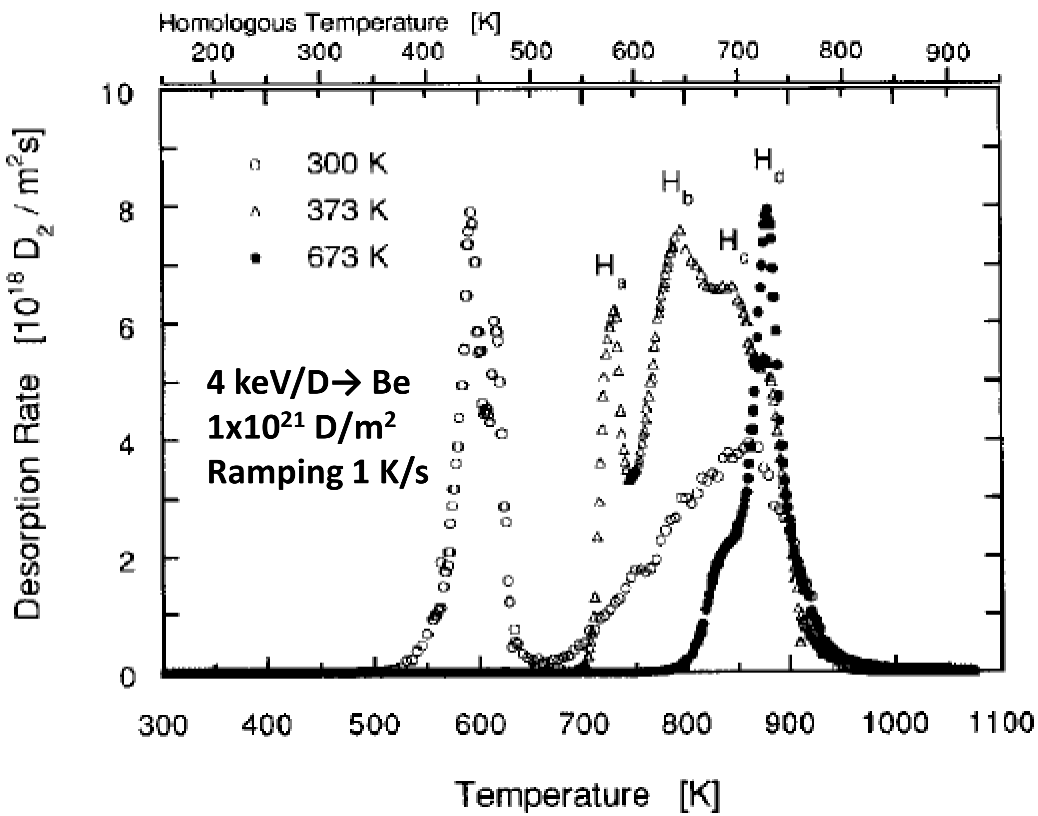

Hydrogen retention of Be alloy developed as neutron multiplier materials

Beryllium metal has some disadvantages for high temperature (600-900 C) DEMO reactor applications, such as low melting temperature, high chemical reactivity at high temperatures.

Candidates are $Be_{12}Ti$, $Be_{12}V$ and $Be_{12}Mo$. Ti, V, and Mo give lower radio activation and high melting temperatures. Be12X structure gives good oxidation resistance and high beryllium content for the neutron multiplier.

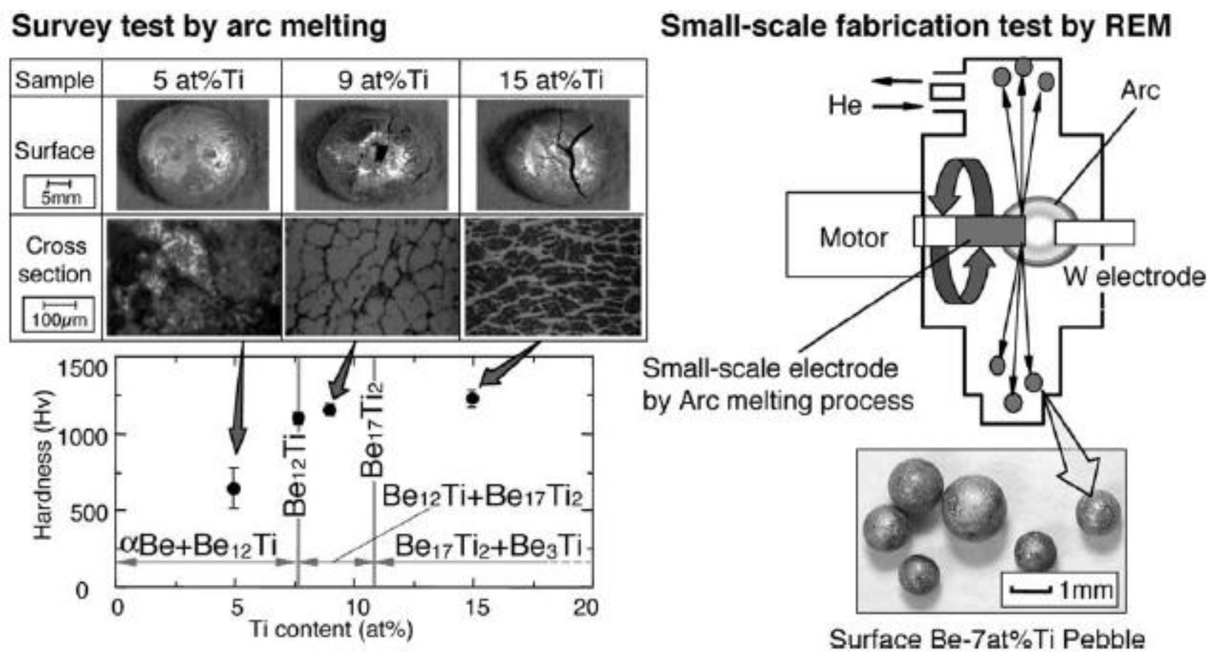

Kuwamura et al., Present status of beryllide R&D as neutron multiplier, JNM 329-333 (2004)

Low hydrogen retention and desorption at lower temperature in $Be_{12}Ti$

Kuwamura et al., JNM329-333 (2004)

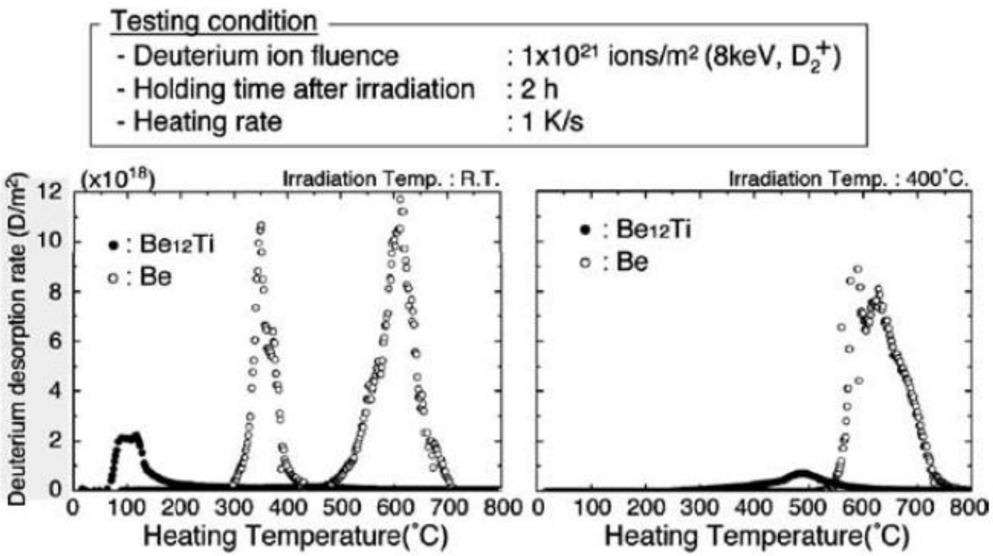

Fig. 8. Results of deuterium release test on heating of implanted $Be_{12}Ti$ and Be.

Mishima et al., JNM367-370 (2007).

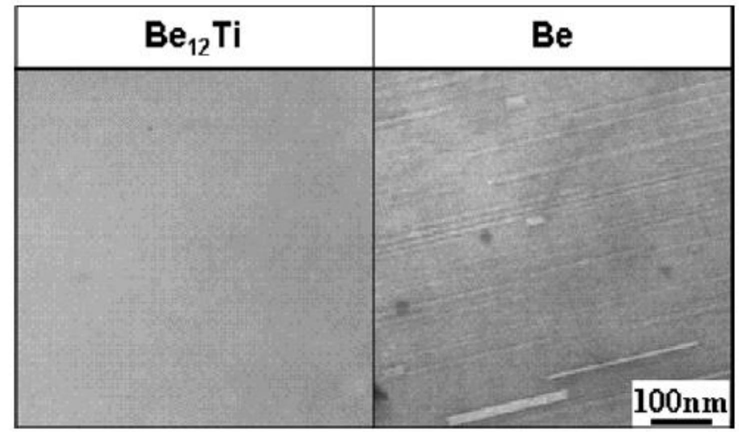

Fig. 6. Transmission-electron micrograph of $Be_{12}Ti$ and beryllium irradiated with 8 keV-D_2^+ to dose of 2×10^{21} D^+/m^2 at 400 °C.

Trapping sites in $Be_{12}Ti$ may be small (< a few nm size) vacancy clusters and impurities.

Neutron irradiation ($4x10^{24}$ n/m^2, > 1MeV, 500 C) on the $Be_{12}Ti$ specimens has been performed at Japan Materials Testing Reactor (JMTR). Tritium inventory in n-irradiated $Be_{12}Ti$ specimen was smaller than that in n-irradiated Be.

Hydrogen isotope retention data research activities in Japan

- Be alloy for blanket materials development will be studied intensively in ITER-BA (centered at IFERC, Rokkasho, Aomori).
- Neutron irradiation effects (knock-on defect, helium transmutation) are key issues in future studies.
- Simulation studies on radiation induced microstructure development and hydrogen trapping are encouraged.